

Strong collective currents of gold nanoparticles in an optical vortex lattice

R. Delgado-Buscalioni,^{1,2,*} M. Meléndez,¹ J. Luis-Hita,^{2,3} M. I. Marqués,^{2,4,5} and J. J. Sáenz^{3,6}

¹*Department of Theoretical Condensed Matter Physics,
Universidad Autónoma de Madrid, 28049 Madrid, Spain*

²*Condensed Matter Physics Center (IFIMAC), Universidad Autónoma de Madrid, 28049 Madrid, Spain*

³*Donostia International Physics Center (DIPC),*

Paseo Manuel Lardizabal 4, 20018 Donostia-San Sebastian, Spain

⁴*Department of Material Physics, Universidad Autónoma de Madrid, 28049 Madrid, Spain*

⁵*Instituto Nicolás Cabrera, Universidad Autónoma de Madrid, 28049 Madrid, Spain*

⁶*IKERBASQUE, Basque Foundation for Science, 48013 Bilbao, Spain*

(Dated: today)

Gold nanoparticles moving in aqueous solution under a optical vortex lattice are shown to present a complex collective optofluidic dynamics. Above a critical field intensity and concentration the system presents a spontaneous transition towards synchronised motion, driven by nonconservative optical forces, thermal fluctuations and hydrodynamic pairing. The system exhibits a rich assortment of collective dynamics such as strong unidirectional currents of nanoparticles at speeds of centimetres per second. This relatively simple optofluidic setup offers an alternative way to control mass and heat transport at the nanoscale, which has been so far elusive.

Efficient transport of nanoscale objects is a very active area of research where optofluidics is heavily involved [1]. Beyond Optical Tweezers [2], light forces induced by stochastic optical fields [3–5] can be used to “activate” and control nanoparticle motion. Optically active micron-sized particles interacting in a time-varying fluctuating speckle light field can diffuse about three times faster than thermally, moving at microns per second [3, 4]. However, below microns, active control becomes elusive due to strong thermal fluctuations [6].

A clever setup has recently been tested [1] using plamon-enhanced optical trapping to fix nanoantennas in microscopic arrangements. In conjunction with an oscillating electric field, photo-induced heating of these nanoantennas leads to microscale natural convection of the surrounding liquid at velocities of tens of $\mu\text{m/s}$ [1]. The driving mechanisms in these previous examples are either of stochastic origin (random speckle patterns) [3, 4] or deterministic (buoyancy) [1].

Instead, *self-organized collective motion* [7] is inspiring new designs of micron-size “artificial swarms” [6, 8, 9] following the ubiquitous examples nature offers (bacteria, ants, birds and more [7, 10]). Its universality is revealed by toy-models, such the as Vicsek model [7], based on extremely simple individual-activation and interaction rules. Hydrodynamics provides a powerful interaction kernel affecting, for example, the complex rotational dynamics of particles [11], often leading to swarming [7]. The “colloidal rollers” are a recent example outside optofluidics. They consist in micron-sized spheres in suspension which, activated by electric [9] or magnetic [8] fields, rotate near a surface and can self-organize into flocks with cluster-speeds of centimetres per second [8].

In this *Letter* we present a new class of optically controlled active media on *time stationary* optical curl-force fields [12–18] acting on a suspension of gold *nanoparti-*

cles (NP). In accordance with self-organized critical phenomena, NPs spontaneously synchronize moving coherently in unidirectional currents at speeds of cm/s . We have numerically investigated these optofluidic dynamics by developing accurate Brownian hydrodynamics solvers which resolve the optical force from the incident light and the many-body forces induced by the light scattered by each NP. The proposed setup is relatively simple and we hope that the striking results presented here will foster experimental work on this subject.

We consider a suspension of N gold NPs of $R = 50$ nm radius in water at dilute volume fraction ($\phi = 4\pi R^3 N / (3V) \sim 10^{-4}$) exposed to an optical field formed by the intersection of two perpendicular coherent laser beams [12, 13] pointing in the x and y directions (optic plane) polarized along z with a phase difference $\theta = \pi/2$ rad (see Fig. 1). This *primary* field with wavelength λ and wavenumber $k = 2\pi/\lambda$ equals $\mathbf{E}_0(\mathbf{r}) = i2|E_0|(\sin(kx) + e^{i\theta}\sin(ky))\hat{\mathbf{z}}$ with $|E_0|^2 = 2In/(c\epsilon\epsilon_0)$ controlled by the intensity of the laser beam I and the refractive index of water $n = \sqrt{\epsilon}$ (ϵ is the relative permittivity and c is the vacuum speed of light). The electrodynamic response of spherical nanoparticles, much smaller than the laser wavelength $R \ll \lambda$, can be well described by their complex electrical polarizability $\alpha = \alpha' + i\alpha''$ (see Supplemental Material, SM). The spatially modulated field \mathbf{E}_{exc} will induce a dipole $\mathbf{p}_i = \epsilon\epsilon_0\alpha\mathbf{E}_{\text{exc}}(\mathbf{r}_i)$ centered on the position of each particle \mathbf{r}_i and, consequently, a non-vanishing averaged Lorentz force with components $\mathbf{F}(\mathbf{r}_i) = (\epsilon\epsilon_0/2)\text{Re}\{\alpha[\mathbf{E}_{\text{exc}}(\mathbf{r}) \cdot \nabla\mathbf{E}_{\text{exc}}^*(\mathbf{r})]\}_{\mathbf{r}=\mathbf{r}_i}$. The primary optical force arises from $\mathbf{E}_{\text{exc}} = \mathbf{E}_0$,

$$\begin{aligned} \mathbf{F}^{(1)}(x, y) = & 2\alpha' \frac{n}{c} I \nabla (\sin^2(kx) + \sin^2(ky)) \\ & + 2\alpha'' \frac{n}{c} I \nabla \times [2 \cos(kx) \cos(ky) \mathbf{e}_z]. \end{aligned} \quad (1)$$

This *nonconservative* force field (1) forms a periodic

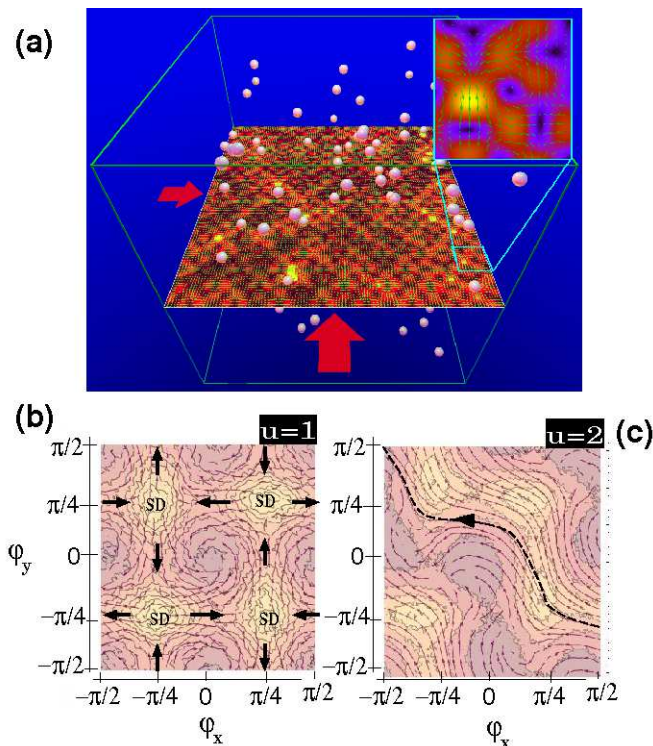


FIG. 1. (a) Suspension of gold nanoparticles of radius $R = 50$ nm in the intersection of two coherent laser beams (red arrows) with $\lambda = 395$ nm polarized in the z (vertical) direction and propagating in the x and y directions (optic plane) with a $\pi/2$ rad phase lag. We show a fixed- z cross section of the force field and the modulus of the total electric field $|E|$ including the incident beams and the light scattered by each NP (brighter regions mean higher $|E|$). In this setup, the NPs remain confined to a cubic box of side $L \simeq 7.0\lambda$. (b) Isocontours of single-particle probability density and streamlines of the NP velocity field in a periodic domain, folded into the Bravais unit cell of the primary optic field $x \in [-\lambda/2, \lambda/2]$ (same for y) against phase-coordinates $\varphi_x = 2\pi(x/\lambda)$. The non-dimensional laser energy (see text) corresponds to $u = 1$ (below) $u = 2$ (above) the transition to coherent NP motion (volume fraction $\phi = 3.0 \times 10^{-3}$). Brighter regions correspond to denser domains. The unstable saddle nodes (SD) of the primary force field (Eq. 1) are indicated in the $u = 1$ panel. The dashed line for $u = 2$ illustrate a zig-zag path followed by NPs under coherent dynamics.

pattern of optical vortices [12], with a Bravais unit cell in $(x, y) \in [-\lambda/2, \lambda/2]$ (see Fig. 1(b)). Its non-conservative part $\nabla \times A(x, y)\hat{z}$, proportional to α'' [19] embodies the so-called “curl forces” [13, 16–18]. It resembles a checkerboard, with alternating squares of positive and negative vorticity. Curl-forces neatly convert the laser energy into work [12, 16, 17] and $U \equiv 2I(n/c)\alpha'' = \epsilon\epsilon_0|E_0|^2\alpha''$ (related to the energy per NP) is a convenient unit to compare with the thermal counterpart $k_B T$. The primary field has no stationary nodes where the NP can rest [15], but four unstable saddle nodes instead (see Fig. 1(b)). As a consequence, an isolated gold NP

experiences giant normal diffusion [14] with a diffusion coefficient $D_{op} \sim \lambda^2/\tau_{op} = u D_{th}$ which is larger than the thermal value D_{th} for $u \equiv U/k_B T > 1$. This non-dimensional laser energy u can be increased up to $\sim 10^2$ before cavitation takes place [20, 21].

We investigate the *collective behaviour* of a *suspension* of gold NPs. Aside from the primary force in Eq. (1) and the thermal kicks, NPs interact optically through multiple scattering forces $\mathbf{F}^{(2)}(\{\mathbf{r}\})$, and also hydrodynamically, with a collective drag velocity $\mathbf{v}_i^{(c)} = \sum_j \mu_{ij}(r_{ij})\mathbf{F}_j$ arising from the *mutual* hydrodynamic mobility μ_{ij} dominated by the Oseen term $\mu_{ij} \sim 1/r_{ij}$.

In order to isolate the effect of hydrodynamic interactions (HI) at fixed ϕ , we first solved these dynamics under periodic boundary conditions (PBC), without taking into account multiple scattering. These dynamics were solved using the Fluctuating Immersed Boundary method (FIB), which is an immersed boundary method for Stokesian particles in fluctuating hydrodynamics [22] (see SM). We evaluate the (time-dependent) single particle diffusion defined as, $D(t) = \Delta_1^2/(4t)$ where $\Delta_1^2 = \langle (\mathbf{r}_1^{\parallel}(t_0 + t) - \mathbf{r}_1^{\parallel}(t_0))^2 \rangle$ is the in-plane (\parallel) mean square displacement (MSD) of a tracer NP with position $\mathbf{r}_1 = \mathbf{r}_1^{\parallel} + z_1\hat{e}_z$. At a fixed ϕ , Fig. 2(a) shows a sudden transition from (enhanced) normal diffusion $D = D_{op}$ to superdiffusion $D(t) \sim t^\beta$, where the diffusion exponent jumps to the ballistic value $\beta = 1$ above the critical laser energy $u > u_{cr}(\phi)$. In periodic boundaries, the superdiffusive regime corresponds to a large current of NPs occupying the whole box in the z direction and flowing with vorticity in $\mathbf{d} = (\pm 1, \pm 1)$ direction. This *3D roll*, illustrated in Fig. 2(c), would be qualitatively similar in an enclosure with walls.

The phase diagram of Fig. 2(d) draws the critical line (u_{cr}, ϕ_{cr}) separating uncorrelated walkers from the synchronized flow of NPs. Beyond, at larger u or ϕ , an extremely rich collective dynamics unfolds (more details in SM). The critical line satisfies $\xi^* = (u_{cr} - u^*)(\phi_{cr} - \phi^*)$ where u^* and ϕ^* are threshold values below which the transition does not occur. Under PBC we find $\xi^* = (1.55 \pm 0.05) \times 10^{-4}$ while $\phi^* = (1.5 \pm 0.1)^{-4}$ and $u^* = 1.0$. Interestingly, coherent dynamics cannot ensue unless the energy per NP surpasses the thermal energy $U > U^* \simeq k_B T$. Also remarkable, is the low threshold concentration ϕ^* involving an average separation of 3λ between NPs.

To investigate the effect of multiple scattering we calculate the many-body secondary optic forces $\mathbf{F}_2(\mathbf{r})$ (see SM) and plugged them into a Brownian solver implemented with the Rotne-Prager-Yamakawa mobility tensor for HI [23]. To fix ϕ we first considered a confined domain where a repulsive external potential impedes NPs from escaping out from a cubic box of side $L = 7\lambda$. This confined geometry mimics an experimentally feasible laser-trap [24]. In this case we analyzed

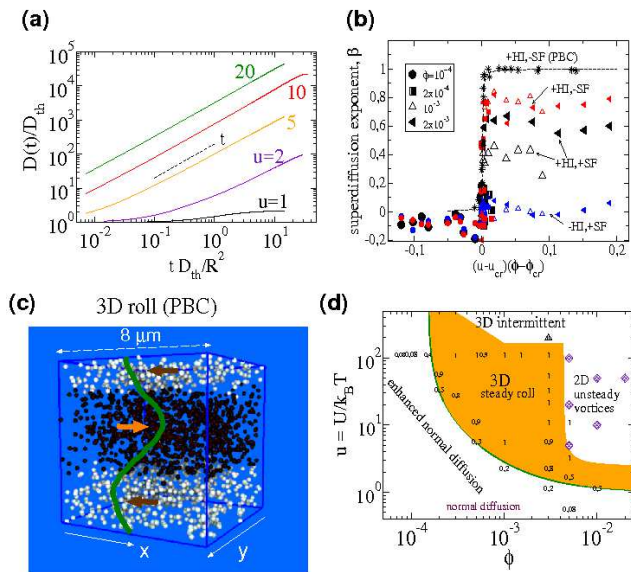


FIG. 2. (a) Effective diffusion coefficient of gold NPs $D(t) = \Delta_1^2/(4t)$ in periodic boundaries at $\phi = 2 \times 10^{-3}$, obtained from single-particle in-plane MSD $\Delta_1^2(t)$ and scaled with the thermal value $D_{th} = k_B T / (6\pi\eta R)$. For $U/K_B T = u > u_{cr} \sim 1$ the dynamics become ballistic $D \sim t^\beta$ with $\beta = 1$. (c) The superdiffusion exponent β against $\xi = [u - u_{cr}(\phi)][\phi - \phi_{cr}(u)]$ for periodic (star symbols) and confined setups. Results with and without hydrodynamic interactions (+HI and -HI) and/or secondary optical forces (+SF and -SF) are compared. (c) The coherent *3D roll* of NPs recirculating in the periodic domain with a sinusoidal velocity profile in the z direction. (d) Dynamic phase diagram showing the transition from enhanced normal diffusion ($D \simeq u D_{th}$) to coherent dynamics $D \sim t^\beta$ at the (green) critical line $\xi^* = (u_{cr} - u^*)(\phi_{cr} - \phi^*)$ (see text for details).

the collective diffusion evaluated from the in-plane displacement of the center of mass (CoM) of the NP ensemble $D_{cm}(t) = \Delta_{cm}^2(t)/(4t)$ (details in the SM). Under confinement, the onset of the superdiffusive regime $D_{cm} \sim t^\beta$ matches the findings under PBC, highlighting the hydrodynamic nature of the transition. Figure 2(b) plots values of β (for both periodic and confined domains) against the governing non-dimensional group $\xi \equiv [u_{cr}(\phi) - u][\phi_{cr}(u) - \phi]$. The transition is sharp and resembles the first-order dynamic transition reported for the Vicsek model [25]. Confinement increases the value of the critical parameter to $\xi^* = (6 \pm 1) \times 10^{-4}$, but it does not alter the shape of the critical line nor significantly modify the threshold values ($u^* \simeq 0.7$ and $\phi \simeq (1.1 \pm 0.01) \times 10^{-4}$), suggesting a sort of “material property”, as in the collective dynamics of micro-rollers [9].

The “microscopic” origin of the coherent dynamics can be understood by plotting the single-NP probability density $\rho(\mathbf{r})$ and the streamlines of the NP average current, in Fig. 1(c). Above the critical energy [$u = 2$ in Fig. 1(c)], superdiffusion arises as an instability of the basic station-

ary solution $\rho_0(\mathbf{r})$, illustrated in Fig. 1(b) ($u = 1$). The instability is triggered by the collective current $\mathbf{v}^{(c)}$ arising from HI. As shown in 1(b), this current breaks one of the symmetries of the primary optical field (mirrored by $\rho_0(\mathbf{r})$) and creates an average mass flow across the system. The particles tend to follow each other along zig-zag paths which move along one of the four possible diagonal directions of the lattice $\mathbf{d} = (\pm 1, \pm 1)$. This is consistent with hydrodynamic pairing [26] which is known to happen if particles are forced to follow curved paths in a liquid. Note that the instability is degenerate in \mathbf{d} and the NP current might jump from one diagonal to another, after many optical times τ_{op} .

Although the dynamic transition stem chiefly from hydrodynamic interactions (HI) [see case $-HI$ in Fig. 2(b)], secondary forces have a measurable effect in reducing the intensity of the collective current. Secondary forces may be viewed as a self-generated, speckle intensity pattern induced by multiple scattering of light. This pattern disrupts the periodic stationary curl force field, thus reducing the coherence of the zig-zag paths followed by the NP’s under coherent motion [see Fig 3(c)]. The phase lag term $\exp[i\mathbf{k} \cdot \mathbf{r}_{ij}]$ present in the optical Green function (see SM) creates undulating force patterns [5] which become quite complex, even for just two isolated NPs $\mathbf{F}^{(2)} = \mathbf{F}^{(2)}(\mathbf{r}_1, \mathbf{r}_2)$ (see Fig. 3). As illustrated in Fig. 3(a), two NPs in the same optic plane tend to repel each other. In a confined domain (see SM), this leads to the expansion of the NP’s ensemble volume. However, along z , the scatter produces marginally stable domains [$F_z = 0$ and $dF_z/dz < 0$, see Fig. 3(b)]. In suspension, this effect leads to transient layers of NPs separated by roughly $\Delta z \sim 2\lambda$ (SM).

A nontrivial question is what happens if the confinement is removed. As a possible outcome, the extra pressure from secondary forces might destroy coherent motion by inducing a fast dispersion of NPs over the optic plane. We prepared experiments placing NPs in the confined domain, with u and initial concentration $\phi(t = 0)$ above the transition line. Upon removing the confining potential, we immediately observe the formation of a jet of NPs moving at an impressive velocity (see video in SM). The trajectories of single NPs, the CoM displacement and velocity $v_{cm}(t)$ are shown in Fig. 4 for one of the cases considered. The jet moves along one the diagonals \mathbf{d} and its direction remains stable until dispersion (mostly along \mathbf{d} direction) leads to $\phi(t) < \phi_{cr}(u)$ [see Fig. 4(b)]. Notably, the flock disperses much less in z direction when secondary forces are added. As shown in SM, attractive secondary normal forces counterbalance the repulsive Oseen drag in z direction. As shown in Fig. 4(c) and (d), the collective velocity scales like $v_{cm} \propto (\phi - \phi_{cr})^{1/3}$ which differs from that observed in the collective motion of microrollers $v_{cm} \sim (\phi - \phi_{cr})$ [8, 9]. A simple scaling argument unifies both results. In terms of the interparticle distance r_{12} , the leading term in the

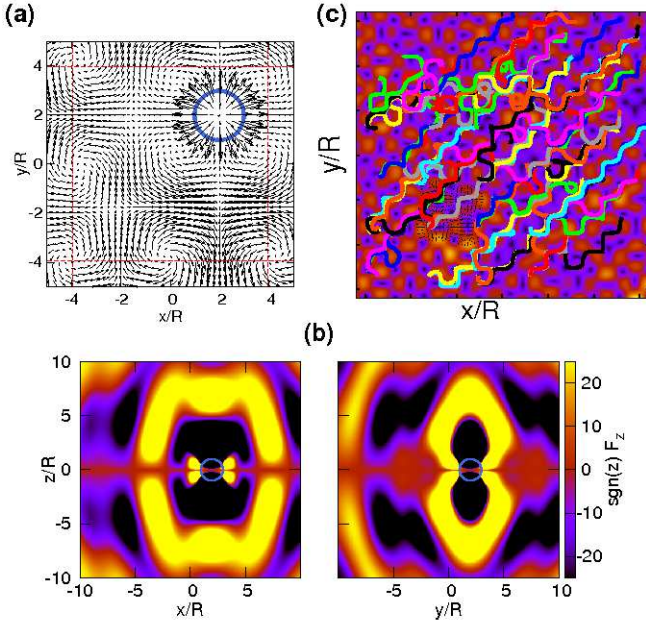


FIG. 3. (a) The force field on particle $i = 2$, in a system with two NPs $\mathbf{F}_2 = \mathbf{F}_2^{(1)}(\mathbf{r}_2) + \mathbf{F}_2^{(2)}(\mathbf{r}_1, \mathbf{r}_2)$, where $\mathbf{F}_2^{(2)}$ comes from the light scattered by NP $i = 1$, located at $z = 0$ and plane location $(1/4, 1/4)\lambda$ (blue circle). The dotted red lines indicate a separation of λ . (b) The corresponding normal component of the optical force F_z in the xz and yz planes times the sign of z . Contours saturate to black (attractive force, $\text{sgn}(z)F_z < 0$) and yellow (repulsive) beyond the values indicated in the colour scale. Red contours, around $z \simeq \pm\lambda = \pm 7.9 R$ correspond to “stable” domains ($F_z = 0$ and $dF_z(z)/dz < 0$). Panel (c) overlaps the trajectories of several NPs moving around the $z = 0$ plane of a confined domain ($L \simeq 2.9 \mu\text{m}$, $\phi = 3 \times 10^{-3}$ and $u = 2$) over the isocontours of the total electric field intensity at the initial time $|E(\mathbf{r}, t_0)|$. Scattering forces induce disruptions of the zig-zag paths and dislocations of the \mathbf{E} lattice pattern.

mutual mobility generally scales like $\mu_{12} \sim 1/r_{12}^\alpha$ while, in a d -dimensional system, $r_{12} \sim \phi^{-1/d}$. One thus expects the collective velocity $v_{cm} \sim \mu_{12}F_2$ to scale like $v_{cm} \sim \phi^{\alpha/d} F$. Groups of microrollers move with $v_{cm} \sim \phi$ [8, 9] close to a wall, where $d = 2$ and $\alpha = 2$. In our setup $d = 3$ and the laser force $F \sim U/\lambda$ activates monopole (Oseen) couplings $\alpha = 1$, providing $v_{cm} \sim \phi^{1/3}U/\lambda$. To complete our scaling, we impose $v_{cm} = 0$ below the critical line, leading to $v_{cm} \propto (u - u_{cr})(\phi - \phi_{cr})^{1/3}$ which agrees quite well with results in periodic, unconfined and confined domains, as shown respectively in (Fig. 4(c), (d) and SM (confined case)).

We have presented a collective dynamic transition of optically driven gold nanoparticles, which shares many generic features of (deterministic) micron-sized active colloidal flocks [8, 9]. By contrast, here, thermal forces are strong but also essential for the enhanced diffusion and the collective dynamics. Without fluctuations the

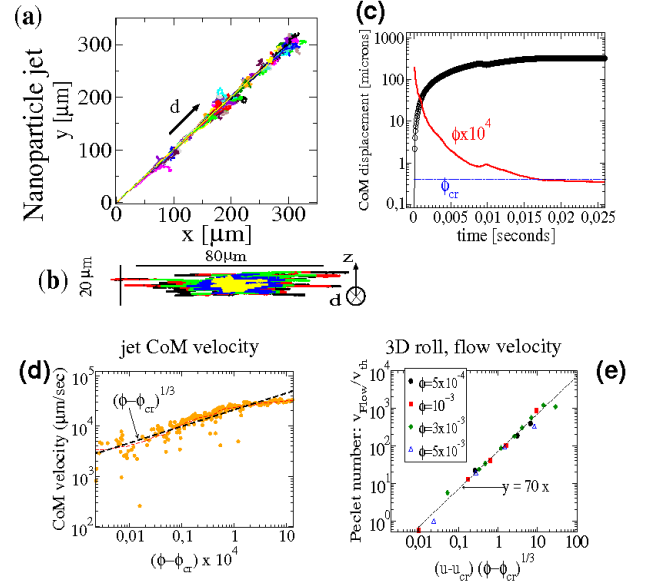


FIG. 4. Nanoparticle jet: (a) Trajectories in the optic plane of 80 nanoparticles after being released from their confinement in a box of $L \simeq 2.9 \mu\text{m}$; the jet moves in direction $\mathbf{d} = \hat{\mathbf{x}} + \hat{\mathbf{y}}$ (different colors for different NPs). (b) Dispersion of the NP’s in the zd plane (colors superpose for increasing times). (c) Displacement of the center of mass (CoM) and (c) the CoM velocity v_{cm} versus the instantaneous volume fraction $\phi(t)$ (measured from the NP’s ensemble volume $\mathcal{V} = \prod_{\alpha} R_{\alpha}^{1/2}$, where \mathbf{R} are the eigenvalues of the ensemble’s gyration tensor). The scaling $v_{cm} \sim (\phi - \phi_{cr})^{1/3}$, showing the peak of the velocity profile of the 3D roll NP-flow (see Fig. 2(c)) in a periodic domain $v_{\text{Flow}} \propto (u - u_{cr})(\phi - \phi_{cr})^{1/3}$

NPs would freeze at the saddle nodes. Calculations under extreme energies $u > 200$, show that NPs take then too long to leave the SD domains, leading to intermittency and suppression of collective motion (see Fig. 2(d) and SM). This is strongly reminiscent of *stochastic resonance* [27] where fluctuations trigger coherent dynamics within a finite window of noise amplitudes. Here, stochastic forces “excite” NP displacements in a *stationary optical field* leading to strong (monopolar) hydrodynamics driving jets of *nanoparticles* at velocities of cm/s, similar to micro-roller clusters [8], but orders of magnitude larger than recent optofluidic setups based on deterministic [1] or stochastic driving [3, 4]. The required power densities are standard for optical tweezers [5] $I \sim 10^9 \text{ W/m}^2$, attained by focusing a 0.1 W laser onto a $\sim 10 \mu\text{m}$ -side domain. Close to the plasmon resonance, local heating is expected upon increasing I [21, 28] so these dynamics might then provide a new way for ultrafast transport of heat at the nanoscale [29]. Also, in our setup the nanoscopic-length Peclet number reaches $\text{Pe} = v_{cm}R\rho_f/\eta \sim 10^2$, promising a novel route for rapid mixing in microdroplets [30].

ACKNOWLEDGEMENTS

We thank Florencio Balboa for his help in the PBC calculations and Raul Pérez for help in RPY implementation. This research was supported by the Spanish Ministerio de Economía y Competitividad (MICINN) and European Regional Development Fund (ERDF) through Projects Explora NANOMIX FIS2013-50510-EXP, FIS2015-69295-C3-3-P, MDM-2014-0377 and the Basque Dep. de Educación through Project PI-2016-1-0041 (J.J.S.). R.D-B acknowledges ACS-PRF grant number 54312-ND9.

* rafael.delgado@uam.es

- [1] J. C. Ndukaiife, A. V. Kildishev, A. G. A. Nanna, V. M. Shalaev, S. T. Wereley, and A. Boltasseva, *Nature Nanotechnology* **11**, 53 (2016).
- [2] P. H. Jones, O. M. Maragó, and G. Volpe, *Optical Tweezers: Principles and Applications* (Cambridge University Press, Cambridge, 2015).
- [3] K. M. Douglass, S. Sukhov, and A. Dogariu, *Nature Photonics* **6**, 834 (2012).
- [4] G. Volpe, G. Volpe, and S. Gigan, *Scientific Reports* **4**, 3936 (2014).
- [5] G. Brügger, L. S. Froufe Pérez, F. Scheffold, and J. J. Sáenz, *Nature Communications* **6**, 7460 (2015).
- [6] C. Bechinger, R. Di Leonardo, H. Löwen, C. Reichhardt, G. Volpe, and G. Volpe, *Reviews of Modern Physics* **88**, 045006 (2016).
- [7] T. Vicsek and A. Zafeiris, *Physics Reports* **517**, 71 (2012).
- [8] M. Driscoll, B. Delmotte, M. Youssef, S. Scanna, A. Donev, and P. Chaikin, *Nature Physics* **13**, 375 (2017).
- [9] A. Bricard, J.-B. Caussin, N. Desreumaux, O. Dauchot, and D. Bartolo, *Nature* **503**, 95 (2013).
- [10] G. Theraulaz, E. Bonabeau, S. C. Nicolis, R. V. Solé, V. Fourcassié, S. Blanco, R. Fournier, J.-L. Joly, P. Fernández, A. Grimal, et al., *PNAS* **15**, 9645 (2002), URL <http://europepmc.org/articles/PMC124961>.
- [11] O. Brzobohatý, A. V. Arzola, M. Šiler, L. Chvátal, P. Jákł, S. Simpson, and P. Zemánek, *Optics Express* **23**, 7273 (2015).
- [12] A. Hemmerich and T. Hänsch, *Physical review letters* **68**, 1492 (1992).
- [13] S. Albaladejo, M. I. Marqués, M. Laroche, and J. J. Sáenz, *Physical Review Letters* **102**, 113602 (2009).
- [14] S. Albaladejo, M. I. Marqués, F. Scheffold, and J. J. Sáenz, *Nanoletters* **9**, 3527 (2009).
- [15] I. Zapata, S. Albaladejo, J. M. R. Parrondo, J. J. Sáenz, and F. Sols, *Physical Review Letters* **103**, 130601 (2009).
- [16] M. V. Berry and P. Shukla, *Journal of Physics A: Mathematical and Theoretical* **46**, 422001 (2013).
- [17] M. V. Berry and P. Shukla, *Proceedings of the Royal Society of London A: Mathematical, Physical and Engineering Sciences* **471** (2015).
- [18] I. Zapata, R. Delgado-Buscalioni, and J. J. Sáenz, *Phys. Rev. E* **93**, 0621130 (2016).
- [19] To maximize the ratio $|\alpha''|/|\alpha'|$ we consider a wavelength close to the gold plasmon resonance in water $\lambda \approx 395$ nm, setting $\epsilon = 1.8$, $\alpha' \approx 1 \times 10^{-21} \text{ m}^3$ and $\alpha'' \approx 2\alpha'$.
- [20] Y. Sivan and S.-W. Chu, *Nanophotonics* **6**, 317 (2017).
- [21] Y. Seol, A. E. Carpenter, and T. T. Perkins, *Optics letters* **31**, 2429 (2006).
- [22] S. Delong, F. B. Usabiaga, R. Delgado-Buscalioni, B. E. Griffith, and A. Donev, *The Journal of chemical physics* **140**, 134110 (2014).
- [23] D. L. Ermak and J. McCammon, *J. Chem. Phys.* **69**, 1352 (1978).
- [24] M. Dienerowitz, M. Mazilu, P. J. Reece, T. F. Krauss, and K. Dholakia, *Optics Express* **16**, 4991 (2008).
- [25] G. Gregoire and H. Chate, *Phys. Rev. Lett.* **92**, 025702 (2012).
- [26] Y. Sokolov, D. Frydel, D. G. Grier, H. Diamant, and Y. Roichman, *Physical review letters* **107**, 158302 (2011).
- [27] L. Gammaitoni, P. Hänggi, P. Jung, and F. Marchesoni, *Reviews of Modern Physics* **70**, 223 (1998).
- [28] O. A. Yeshchenko, N. V. Kutsevol, and A. P. Naumenko, *Plasmonics* **11**, 345 (2016).
- [29] G. Baffou and R. Quidant, *Laser & Photonics Reviews* **7**, 171 (2013).
- [30] W. H. Chong, L. K. Chin, R. L. S. Tan, H. Wang, A. Q. Liu, and H. Chen, *Angew. Chem. Int. Ed.* **52**, 8750 (2013).